ties (Fig. 2). To investigate these in greater detail, we resampled a portion of the Taylor Dome record at higher resolution for chloride and compared it with the GISP2 chloride series. Their variability is equivalent (within a factor of 2), and both display similar style abrupt change events. The onset of the YD in the GISP2 record occurs in less than 20 years (*8*, *18*), and although not as well dated, the onset of the ACR in the Taylor Dome record also appears to be rapid (Fig. 2). Mean chloride concentration during the YD in Greenland is 75% of the maximum late glacial value, whereas the ACR at Taylor Dome (Fig. 2) is 54% of the last glacial maximum value, consistent with results from Dome B (*5*). Although it is tempting to correlate specific, decade-to-century–scale, rapid change events, the control of dating on the Taylor Dome is not equivalent to that of the GISP2 series.

From <10,000 to 14,600 years ago, Southern Hemisphere polar atmospheric circulation was not extensive enough to incorporate significant amounts of dust from ice-free continents of the Southern Hemisphere despite arid conditions during at least portions of the YD-ACR periods in regions such as Africa (*19*). However, atmospheric circulation was vigorous enough to increase the transport of sea salt to Antarctica. Fluctuations in the size of this atmospheric circulation system are recorded in the Taylor Dome chloride series. This series displays variability and a general sequence of events (a YD equivalent or an ACR plus several other rapid change events) that are very similar to events characterizing the deglaciation record in Greenland ice cores. The diversity of events displayed in the Taylor Dome chloride series may not have been observed in previous Antarctic stable isotope or dust series because of the resolution of these records or because these events were largely restricted to change over the Antarctic Ocean. Because modern sea-salt concentrations decline markedly with distance inland from the coast, sites such as Taylor Dome would be expected to contain a more complete record of fluctuations in sea salt. Glaciochemical series provide a measure of atmospheric circulation (*14*, *15*) and not of regional surface temperature, as do stable isotopes (*20*). Thus, glaciochemical series provide a compatible view of climate change, recording migrations of atmospheric circulation over continents and oceans.

We conclude, on the basis of our comparison of Taylor Dome and GISP2 ice core records, that similar-scale fluctuations of atmospheric circulation occurred over both northern and southern polar marine areas during at least the deglaciation. Fluctuations in temperature over Antarctica and Greenland may not have been as similar, perhaps because of the dramatically different degree of change in ice cover over these two regions. The origin and detailed phasing of the events compared in this study are still unknown, leaving open the question of a forcing mechanism. However, we now have a demonstration that events similar in variability to those seen in Greenland ice cores do exist in Antarctic ice core records.

REFERENCES AND NOTES

1. F. Gasse *et al.*, *Quat. Res.* **32**, 229 (1989); J. T. Overpeck *et al.*, *Nature* **338**, 553 (1989).
2. G. H. Denton and C. H. Hendy, *Science* **264**, 1434 (1994).
3. J. T. Heine, *Quat. Sci. Rev.* **12**, 769 (1993).
4. J. Jouzel *et al.*, in *The Last Deglaciation: Absolute and Radiocarbon Chronologies* vol. 2 of *NATO ASI Series I*, E. Bard and W. S. Broecker, Eds. (Springer-Verlag, Berlin, Heidelberg, 1992), pp. 230–266.
5. J. Jouzel *et al.*, *Clim. Dyn.* **11**, 151 (1995).
6. P. M. Grootes *et al.*, *Eos* **75**, (no. 44), 225 (1994); P. M. Grootes, E. J. Steig, M. Stuiver, E. D. Waddington, D. L. Morse, in preparation.
7. E. D. Waddington, D. L. Morse, P. M. Grootes, E. J. Steig, in *Ice in the Climate System* vol. 12 of *NATO ASI Series I*, W. R. Peltier, Ed. (Springer-Verlag, Berlin, Heidelberg, 1993), pp. 499–516; B. Malaize *et al.*, *Eos* **75** (no. 44), 226 (1994); E. J. Steig *et al.*, in preparation.
8. R. B. Alley *et al.*, *Nature* **362**, 527 (1993).
9. D. A. Meese *et al.*, *Preliminary Depth-Age Scale of the GISP2 Ice Core* (Cold Regions Research and Engineering Laboratory Technical Report number 94-01, Hanover, NH, 1994).
10. M. Stuiver, P. M. Grootes, T. F. Braziunas, *Quat. Res.* **44**, 341 (1995).
11. A. Ruddiman and A. McIntyre, *Palaeogeogr. Palaeoclimatol. Palaeoecol.* **35**, 145 (1981); E. Bard *et al.*, *Quat. Res.* **31**, 309 (1989); L. D. Keigwin, G. A. Jones, S. J. Lehman, *J. Geophys. Res.* **96**, 16811 (1991).
12. M. DeAngelis, N. I. Barkov, V. N. Petrov, *J. Atmos. Chem.* **14**, 233 (1992).
13. J. R. Petit, M. Briat, A. Royer, *Nature* **293**, 391 (1981).
14. P. A. Mayewski *et al.*, *Science* **261**, 195 (1993).
15. P. A. Mayewski *et al.*, *ibid.* **263**, 1747 (1994).
16. H. Enomoto, *Clim. Change* **18**, 67 (1991).
17. E. Cook *et al.*, *Science* **253**, 1266 (1991).
18. K. C. Taylor *et al.*, *Nature* **361**, 432 (1992).
19. F. Gasse, *ibid.* **265**, 42 (1977); J. C. Stager, *Quat. Res.* **29**, 54 (1988).
20. C. Lorius and L. Merlivat, *IAHS Publication no. 118*, 125 (1977).
21. T. Nilsson, *The Pleistocene Geology and Life in the Quaternary Ice Age* (D. Reidel, Dordrecht, Netherlands, 1983).

22. We thank the NSF for financial support of the GISP2 and Taylor Dome ice core projects. We also thank the drillers from the Polar Ice Coring Office University of Alaska, notably D. Giles and M. Wumkes; the Antarctic Support Associates personnel for camp support and logistics; Squadron VXE6 and the New York Air National Guard (TAG 109) for air support; the GISP2 Science Management Office (University of New Hampshire); and field party members for their able assistance.

5 October 1995; accepted 4 April 1996

Melting of $H_2SO_4 \cdot 4H_2O$ Particles upon Cooling: Implications for Polar Stratospheric Clouds

Thomas Koop and Kenneth S. Carslaw

Polar stratospheric clouds (PSCs) are important for the chemical activation of chlorine compounds and subsequent ozone depletion. Solid PSCs can form on sulfuric acid tetrahydrate (SAT) ($H_2SO_4 \cdot 4H_2O$) nuclei, but recent laboratory experiments have shown that PSC nucleation on SAT is strongly hindered. A PSC formation mechanism is proposed in which SAT particles melt upon cooling in the presence of HNO_3 to form liquid HNO_3-H_2SO_4-H_2O droplets 2 to 3 kelvin above the ice frost point. This mechanism offers a PSC formation temperature that is defined by the ambient conditions and sets a temperature limit below which PSCs should form.

Nitric acid–containing polar stratospheric clouds (type 1 PSCs) are typically observed at temperatures below 196 K (*1*). Their formation leads to a considerable increase in aerosol surface area and therefore in the rates of important heterogeneous reactions. Despite their importance, the composition and formation mechanisms of type 1 PSCs are not completely understood (*2*). It is now recognized that background liquid aerosols absorb large amounts of HNO_3 with decreasing temperature and grow into liquid HNO_3-H_2SO_4-H_2O PSCs (*3*–*5*). Alternatively, all, or at least a fraction, of the background nuclei for PSC growth can be solid, most likely SAT. Sulfuric acid tetrahydrate is frequently observed in laboratory experiments (*3*, *6*–*8*), and the existence of H_2SO_4-containing solids in the stratosphere has been inferred from observations (*9*). Once formed, SAT particles can persist to temperatures as high as 210 to 215 K, above which they melt to form H_2SO_4-H_2O droplets (*6*).

Because SAT particles are stable over a wide temperature range, they are likely to persist for long periods. Therefore, it is essential to understand how PSCs form when they act as the condensation nuclei. The

Max Planck Institute for Chemistry, Postfach 3060, 55020 Mainz, Germany.

PSC formation mechanism included in most models involves nucleation of nitric acid trihydrate (NAT) ($HNO_3 \cdot 3H_2O$) on SAT (*1*). However, recent laboratory experiments (*8*) and calculations (*10*) under stratospheric conditions have suggested that the nucleation of NAT on SAT is very strongly inhibited, requiring supercooling by up to 8 K (*8*). This constraint would imply that once SAT particles have formed, the frequency with which type 1 PSCs occur would be reduced significantly (*8*), thus affecting polar ozone depletion. However, with a thermodynamic model, it can be shown that SAT particles become unstable and transform into much larger ternary liquid HNO_3-H_2SO_4-H_2O droplets upon cooling, thus providing a pathway for type 1 PSC formation at a defined temperature.

The conditions under which H_2SO_4 solid phases form and persist can be determined by examining the composition of stratospheric H_2SO_4-H_2O droplets and the melting points of the different solid phases (*11*) (Fig. 1A). For temperatures lower than the melting point, liquid aerosols are supersaturated (supercooled) with respect to the solid. A useful measure of the supersaturation is the saturation ratio S (*12*) (Fig. 1B). Solid particles are stable with respect to liquids when $S > 1$ but are unstable when $S < 1$. For example, a stratospheric sulfuric acid monohydrate (SAM) ($H_2SO_4 \cdot H_2O$) particle is stable in air (with a water partial pressure of 2.5×10^{-4} mbar) between about 266 and 216 K (Fig. 1), and SAT is stable between about 213 and 188 K. Laboratory experiments have shown that SAT can transform into liquid H_2SO_4-H_2O (with composition at point a in Fig. 1) by warming above about 210 to 215 K (*6*), and SAM can melt or deliquesce upon cooling below about 220 K (*13*) (point b) (deliquescence is a solid-to-liquid transformation involving the transfer of vapor from or to the gas phase). Cooling of SAT below about 188 K (point c) would lead to ice formation instead of deliquescence because SAT becomes unstable only below the ice frost point (point d) under stratospheric conditions.

However, liquid stratospheric aerosols absorb considerable amounts of HNO_3 at low temperatures (*3–5*), which can completely change the behavior of SAT particles upon cooling. The saturation ratio with respect to SAT in ternary liquid HNO_3-H_2SO_4-H_2O droplets under typical stratospheric conditions was calculated as a function of temperature (Fig. 2A). The presence of HNO_3 in the droplets (Fig. 2B) significantly reduces SAT stability. In air containing H_2O and HNO_3, SAT is stable with respect to the ternary liquid for temperatures higher than point 1 (and therefore remains "dry") but is unstable at lower temperatures. At point 1, SAT can coexist in equilibrium with a ternary liquid ($S = 1$), so cooling of an initially dry SAT particle to point 1 leads to deliquescence (*14*). At the initial point of deliquescence (point 1), all of the HNO_3 is still in the gas phase, so the liquid film that begins to form on SAT has the composition of a pure liquid droplet in equilibrium with a gas phase undepleted in HNO_3 (in this case, 47 weight % HNO_3 and 3 weight % H_2SO_4) (Fig. 2B). Upon further cooling, SAT continues to dissolve (thick solid line) as more HNO_3 and H_2O is partitioned from the gas phase into the liquid. The SAT completely dissolves at point 2, and with further cooling, the composition of the pure liquid droplets continues to follow the thick dashed line (Fig. 2B).

Deliquescence simply arises as a result of the thermodynamic instability of SAT with respect to the ternary solution. One proposed type I PSC formation mechanism involves nucleation of a binary HNO_3-H_2O solution on SAT (*5*, *10*) followed by heterogeneous NAT nucleation. Although amorphous HNO_3-H_2O phases have been observed to nucleate on glass or silicon surfaces in laboratory studies (*15*), SAT is not an inert substrate and cannot coexist at thermodynamic equilibrium with a binary liquid HNO_3-H_2O layer. This restriction excludes the nucleation of a liquid because at the moment of formation a critical embryo is required to be in equilibrium with the supporting nucleus.

Without HNO_3 in the gas phase, SAT becomes unstable only below the ice frost point (point d in Figs. 1 and 2). The change in water partial pressure associated with ice growth (even on a fraction of the particles) prevents the remaining SAT particles from deliquescing. The transformation of SAT to a liquid at these low temperatures is therefore only possible in the presence of HNO_3. Although SAT is usually the stable H_2SO_4 solid phase in the stratosphere, sulfuric acid hemihexahydrate (SAH) ($H_2SO_4 \cdot 6.5H_2O$)

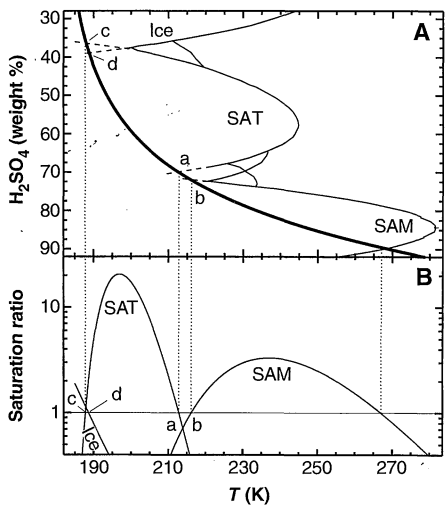

Fig. 1. (**A**) Concentration of stratospheric H_2SO_4-H_2O droplets (thick solid line) in equilibrium with a water partial pressure of 2.5×10^{-4} mbar [equivalent to 5 parts per million by volume (ppmv) at a 50-mbar altitude] superimposed on the H_2SO_4-H_2O phase diagram. Melting points of the different solid phases are indicated by thin solid lines (*11*). Solid phases are SAM (sulfuric acid monohydrate), SAT (sulfuric acid tetrahydrate), and ice. Melting points of other minor solid phases ($H_2SO_4 \cdot 2H_2O$, $\cdot 3H_2O$, and $\cdot 6.5H_2O$) are also shown. (**B**) Saturation ratio S with respect to SAT, SAM, and ice. Point d is the ice frost point. Although stratospheric SAT particles are "dry" between 213 K (point a) and 188 K (point c), the composition (A) and saturation ratio (B) in a liquid droplet under the same conditions can be used to determine conditions where SAT particles are stable. The equilibrium droplet composition and saturation ratios were calculated from the thermodynamic model of Carslaw *et al.* (*20*).

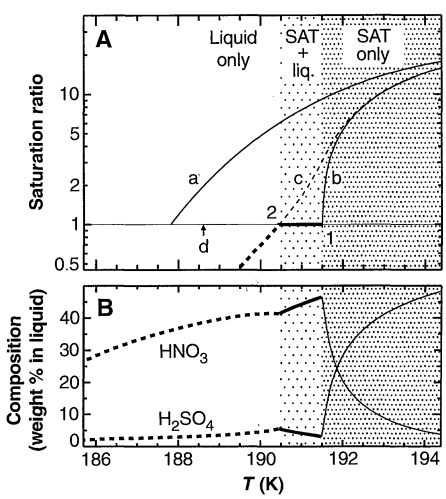

Fig. 2. (**A**) Saturation ratio S of liquid stratospheric aerosols with respect to SAT. (**B**) Composition of liquid. As in Fig. 1, the stability of dry SAT particles can be determined by examining S in liquid droplets that would exist under the same conditions. Line a: pure H_2SO_4-H_2O droplets (as in Fig. 1), line b: ternary HNO_3-H_2SO_4-H_2O droplets at 50-mbar altitude in equilibrium with 5 ppmv of H_2O and a fixed HNO_3 gas phase of 10 ppbv [liquid composition, thin solid line in (B)], line c: same as line b, except with a constant total HNO_3 amount, allowing for partitioning of HNO_3 into the droplets. In the densely shaded region, SAT particles are stable and therefore remain "dry." Point 1 is the deliquescence temperature of SAT where $S = 1$. Between points 1 and 2 (light shading) a ternary liquid HNO_3-H_2SO_4-H_2O film coexists with SAT [composition, thick solid line in (B)]. At point 2, SAT is completely dissolved, and at lower temperatures, pure liquid HNO_3-H_2SO_4-H_2O droplets exist [thick dashed line in (A) and (B)]. Point d is the ice frost point. All saturation ratios were calculated in terms of solution activities in the ternary solution (*12*). Model calculations are uncertain to within about ±1 K.

might also form. However, SAH would also deliquesce upon cooling at approximately the same temperature as SAT.

An important constraint is that deliquescence must occur before the nucleation of any HNO_3 solid phases. For example, at the deliquescence point, NAT is supercooled to about 4 K below its equilibrium temperature, equivalent to a saturation ratio of 20 to 25. However, laboratory experiments have demonstrated SAT deliquescence occurring rather than NAT nucleation: Iraci *et al.* (*8*) showed that SAT films cooled in the presence of HNO_3 and H_2O vapor developed a noncrystalline layer containing HNO_3 and H_2O (H_2SO_4 was not detected in the layer at their experimental sensitivity). The noncrystalline films could be held under these conditions for several hours without NAT nucleation, even with NAT saturation ratios as high as 127. We believe that these observations are attributable to the slow transformation of SAT into a ternary HNO_3-H_2SO_4-H_2O liquid (*16*). In 7 experiments (from a total of 12), the experimental observations agree with our prediction of deliquescence (either a noncrystalline film was observed below the deliquescence temperature T_d or no film was observed above T_d), and in the remaining 5 experiments, the measured temperature differed from T_d by only 0.3 to 1.3 K, which is within the combined ±1.5 K uncertainty in their experimental conditions and our model calculations. In earlier experiments, Hanson (*17*) studied the uptake of HNO_3 onto SAT and found that enough HNO_3 was adsorbed by the surface at 191.5 K to form the equivalent of about 30 monolayers of HNO_3. The HNO_3 vapor pressure over this growing layer was 10 to 20 times as great as that over NAT, suggesting the growth of a metastable HNO_3 phase (*17*). However, we have calculated that SAT deliquescence would have started below 192.5 K, indicating that this observation was probably the result of formation of a ternary solution on the SAT. The calculated HNO_3 vapor pressure of the resulting ternary solution in equilibrium with SAT is approximately half of that observed experimentally, which again is well within the experimental uncertainties (*18*).

These laboratory observations under stratospheric conditions support our theoretical prediction of SAT deliquescence upon cooling. They also suggest that SAT deliquescence is the preferred phase transition, rather than nitric acid hydrate nucleation from the gas phase, even at high saturation ratios. Therefore, care must be taken in the interpretation of experiments designed to investigate nitric acid hydrate nucleation on SAT or SAH from the gas phase; at temperatures less than the deliquescence point, nucleation in the ternary liquid is likely to be the controlling mechanism. To assist in the interpretation of laboratory experiments and theoretical calculations, we have calculated the SAT deliquescence temperature and the corresponding NAT saturation ratio as a function of HNO_3 and H_2O partial pressures (Fig. 3).

At present, the best indicator of SAT deliquescence in the stratosphere is probably the change in aerosol size with changes in temperature. Deliquescence leads to significant uptake of HNO_3 and H_2O from the gas phase and a consequent steep increase in aerosol volume (Fig. 4). This change in volume of up to a factor of 10 within a temperature interval of only 1 K should be observable in existing and future field measurements.

As a further possibility, we note that rather than the droplets remaining liquid, their growth after deliquescence could initiate nitric acid hydrate nucleation. Although nitric acid hydrate formation in droplets with equilibrium compositions seems unlikely (*7*), rapid growth of the deliquescing SAT particles to form large HNO_3-H_2SO_4-H_2O droplets would lead to strong departures from equilibrium (*19*). In particular, the composition of the smallest particles could approach pure HNO_3-H_2O and cause them to freeze as a nitric acid hydrate (*19*). In contrast to the Meilinger *et al.* (*19*) study, rapid temperature fluctuations would not be needed in our mechanism to induce a strong departure from equilibrium; instead, temperatures would simply have to fall below the deliquescence point. Further laboratory experiments and time-dependent droplet growth calculations are required to answer this question.

Deliquescence of SAT is important not only because it occurs before nitric acid hydrate nucleation but also because it occurs at a well-defined temperature for given abundances of HNO_3 and H_2O (Fig. 3). Moreover, deliquescence sets a temperature limit below which the formation of type 1 PSCs must occur, independent of whether the initial particles are liquid or frozen as known H_2SO_4 hydrates. Even if the background aerosol consists of a mixed population of liquid and solid H_2SO_4 particles, PSC growth must occur at a temperature between the dashed line and the heavy solid line in Fig. 4.

Accurate predictions of PSC formation in the Arctic, where temperatures are often marginal for PSC formation, are a major challenge. One of the greatest obstacles is the uncertainty in the formation temperature of type 1 PSCs in atmospheric models, which is usually assumed to be anywhere between 0 and 4 K below the NAT condensation temperature. Calculations (*4*, *5*) have shown that when the initial background aerosols are liquid, they grow at a well-defined temperature without nucleation. We have shown that when the background aerosols are frozen as known H_2SO_4 hydrates, deliquescence upon cooling also leads to type 1 PSC formation at a defined temperature. This improves considerably our ability to predict the development of PSCs and subsequent ozone depletion.

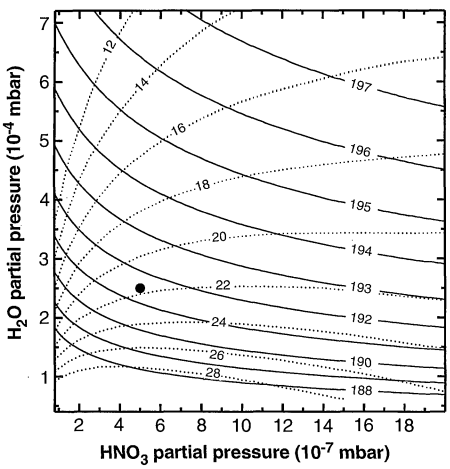

Fig. 3. SAT deliquescence temperatures (solid lines, values in kelvin) and saturation ratios with respect to NAT at the deliquescence point (dotted lines) for typical stratospheric abundances of HNO_3 and H_2O. For temperatures approximately 1 K lower than indicated by the solid lines, SAT transforms completely into HNO_3-H_2SO_4-H_2O liquid. The dot marks the conditions used in Fig. 2.

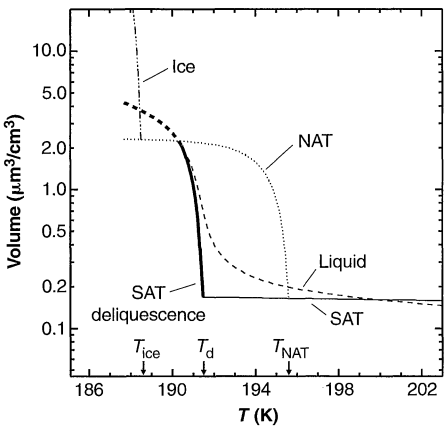

Fig. 4. Equilibrium particle volumes (aerosol volume per unit volume of air) associated with different types of PSCs at 50-mbar altitude with 5 ppmv of H_2O, 10 ppbv of HNO_3, and 0.5 ppbv of H_2SO_4. An H_2SO_4 abundance typical of background (nonvolcanic) conditions was used (0.5 ppbv is equivalent to about 1.5×10^{-13} g/cm³ at 50 mbar and 200 K). Higher H_2SO_4 abundances did not change the deliquescence temperature but did alter the change in volume with decreasing temperature. Ice frost point, T_{ice}; SAT deliquescence point, T_d; and NAT saturation temperature, T_{NAT}.

REFERENCES AND NOTES

1. L. R. Poole and M. P. McCormick, *J. Geophys. Res.* **93**, 8423 (1988).
2. M. A. Tolbert, *Science* **264**, 527 (1994).
3. M. J. Molina *et al.*, *ibid.* **261**, 1418 (1993).
4. K. S. Carslaw *et al.*, *Geophys. Res. Lett.* **21**, 2479 (1994); K. Drdla *et al.*, *ibid.*, p. 2475; A. Tabazadeh, R. P. Turco, M. Z. Jacobson, *J. Geophys. Res.* **99**, 12897 (1994).
5. A. Tabazadeh, R. P Turco, K. Drdla, M. Z. Jacobson, O. B. Toon, *Geophys. Res. Lett.* **21**, 1619 (1994).
6. A. M. Middlebrook *et al.*, *J. Geophys. Res.* **98**, 20473 (1993).
7. T. Koop *et al.*, *Geophys. Res. Lett.* **22**, 917 (1995).
8. L. T. Iraci, A. M. Middlebrook, M. A. Tolbert, *J. Geophys. Res.* **100**, 20969 (1995).
9. J. M. Rosen, N. T. Kjome, S. J. Oltmans, *ibid.* **98**, 12741 (1993); A. Adriani, T. Deshler, G. Di Donfrancesco, G. P. Gobbi, *ibid.* **100**, 25977 (1995).
10. A. R. MacKenzie, M. Kulmala, A. Laaksonen, T. Vesala, *ibid.* p. 11275 (1995).
11. C. M. Gable, H. F. Betz, S. H. Maron, *J. Am. Chem. Soc.* **72**, 1445 (1950).
12. Saturation ratios were calculated from the species activities *a* in solution; for example, the SAT saturation ratio $S = [a(H^+)]^2[a(SO_4^{2-})][a(H_2O)]^4/K$, where K is the activity product of a solution saturated with respect to SAT at temperature T (*20*).
13. R. Zhang, M.-T. Leu, L. F. Keyser, *J. Geophys. Res.* **100**, 18845 (1995).
14. At temperatures higher than the deliquescence point, SAT particles cannot coexist with ternary HNO_3-H_2SO_4-H_2O or binary H_2SO_4-H_2O solutions and therefore remain effectively "dry." Although molecules might become adsorbed on the surface, they cannot grow into liquids in equilibrium with SAT.
15. J. J. Marti and K. Mauersberger, *Geophys. Res. Lett.* **20**, 359 (1993).
16. The time required for the complete deliquescence of SAT is determined by the uptake of HNO_3 to form a ternary solution. With the film geometry and an HNO_3 partial pressure in the range 5×10^{-8} to 8×10^{-7} torr, the uptake time is on the order of the observation time.
17. D. R. Hanson, *Geophys. Res. Lett.* **19**, 2063 (1992).
18. The experimental uncertainty in the partial pressure of HNO_3 is +100/−50%. Also, a 7% decrease in the experimental partial pressure of H_2O, well within the experimental uncertainty of ±20%, would lead to a calculated HNO_3 vapor pressure that was higher by a factor of 2 (in agreement with that observed) in order to maintain equilibrium with SAT.
19. S. K. Meilinger *et al.*, *Geophys. Res. Lett.* **22**, 3031 (1995).
20. K. S. Carslaw, S. L. Clegg, P. Brimblecombe, *J. Phys. Chem.* **99**, 11557 (1995).

21. We thank B. Luo and T. Peter for helpful discussions and are grateful to L. Iraci and R. Zhang for sending us preprints of their work. This work formed part of the thesis of T.K. at the University of Mainz.

6 February 1996; accepted 22 April 1996

Compensatory *ahpC* Gene Expression in Isoniazid-Resistant *Mycobacterium tuberculosis*

David R. Sherman, Khisimuzi Mdluli, Mark J. Hickey, Taraq M. Arain, Sheldon L. Morris, Clifton E. Barry III,* C. Kendall Stover*†

Mutations that eliminate KatG catalase–peroxidase activity prevent activation of isoniazid and are a major mechanism of resistance to this principal drug for the treatment of *Mycobacterium tuberculosis* infections. However, the loss of KatG activity in clinical isolates seemed paradoxical because KatG is considered an important factor for the survival of the organism. Expression of either KatG or the recently identified alkyl hydroperoxidase AhpC was sufficient to protect bacilli against the toxic effects of organic peroxides. To survive during infection, isoniazid-resistant KatG mutants have apparently compensated for the loss of KatG catalase–peroxidase activity by a second mutation, resulting in hyperexpression of AhpC.

As an intracellular pathogen residing within macrophages, *Mycobacterium tuberculosis* (MTB) is well equipped to resist toxic oxygen species. However, a principal drug used to treat tuberculosis, isoniazid (isonicotinic acid hydrazide, or INH) interacts with components of the mycobacterial defense against oxidative stress in complex ways. INH is a prodrug that requires activation to an unstable electrophilic species by the catalase-peroxidase KatG, with hydrogen peroxide (H_2O_2) acting as an electron sink for the reaction (*1–3*). Once activated, INH inhibits the biosynthesis of cell wall mycolic acids (*4*), ultimately compromising the inert and largely impenetrable barrier that protects mycobacteria against reactive oxygen species and other environmental insults (*5*). KatG is the only MTB enzyme capable of activating this drug. As a result, KatG-mutant MTB strains are INH resistant.

Tuberculosis bacteria appear to rely on the constitutive defense afforded by their cyclopropanated cell wall mycolic acids, having virtually eliminated an inducible oxidative stress response from their genetic repertoire (*6*). In other bacteria, a peroxide-inducible genetic response mediated by the transcription factor OxyR is the primary defense against oxidative stress (*7, 8*). However, the recently identified *oxyR* gene of MTB is vestigial, containing numerous frameshifts and deletions (*6, 9*). Without OxyR, the only MTB protein whose expression is peroxide-inducible is KatG, and this induction is insufficient to protect against H_2O_2 challenge (*6*). It therefore seems paradoxical that loss of KatG function is the major means by which the tubercle bacilli acquire resistance to isoniazid (*10, 11*). It is unclear how these bacteria adapt to loss of KatG, their only catalase-peroxidase and their only peroxide-responsive gene product, when this activity is considered an important component of intracellular survival (*12*).

To evaluate the interaction of INH and H_2O_2 in TB-complex bacilli, we simultaneously administered subinhibitory concentrations of both H_2O_2 and isoniazid to *Mycobacterium bovis* BCG (an avirulent member of the TB complex). As in Gram-negative bacteria and the soil saprophyte *Mycobacterium smegmatis* (*13*), synergy was readily apparent. A reduction in cell viability by a factor of 100 was noted after 72 hours exposure to concentrations of H_2O_2 and INH that separately had no effect in this assay (Fig. 1). When subinhibitory concentrations of both agents were supplied to a *katG*-deleted BCG strain, no synergy was observed (*14*). The observed synergy is consistent

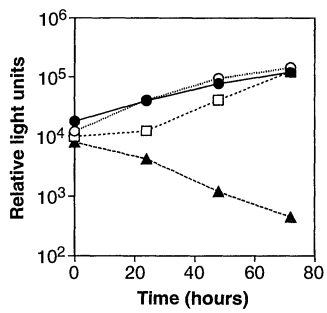

Fig. 1. Synergistic interaction of H_2O_2 and isoniazid. *M. bovis* BCG Connaught (ATCC 35745) transfected with an integrating plasmid constitutively expressing the firefly luciferase (*lux*) gene product (BCG:r361lux) (*23*) was grown at 37°C in 7H9 media supplemented with albumin and dextrose, but in the absence of exogenous catalase (7H9 no cat). Cells were passaged twice at low density [absorbance at 540 nm (A_{540}) ≤ 0.01] before dilution to ~1 × 10^5/ml for treatment. Cell viability was determined by monitoring light expression as described (*23*). (●) No H_2O_2, no INH; (○) no H_2O_2, 0.06 μg/ml INH; (□) 130 μM H_2O_2, no INH; and (▲) 130 μM H_2O_2, 0.06 μg/ml INH.

D. R. Sherman, M. J. Hickey, T. M. Arain, C. K. Stover, Laboratory of Tuberculosis and Molecular Microbiology, PathoGenesis Corporation, 201 Elliott Avenue West, Seattle, WA 98119, USA.
K. Mdluli and C. E. Barry III, Tuberculosis Research Unit, Laboratory of Intracellular Parasites, National Institutes for Allergy and Infectious Diseases, Rocky Mountain Laboratories, Hamilton, MT 59840, USA.
S. L. Morris, Laboratory of Mycobacteria, Center for Biologics Evaluation and Research, Food and Drug Administration, Bethesda, MD 20892, USA.

*These authors contributed equally to this work.
†To whom correspondence should be addressed.